

Quenched Noise and Nonlinear Oscillations in Bistable Multiscale Systems

Christian Kuehn
Technical University of Munich (TUM)

November 27, 2017

Abstract: *Nonlinear oscillators are a key modelling tool in many applications. The influence of annealed noise on nonlinear oscillators has been studied intensively. It can induce effects in nonlinear oscillators not present in the deterministic setting. Yet, there is no theory regarding the quenched noise scenario of random parameters sampled on fixed time intervals, although this situation is often a lot more natural. Here we study a paradigmatic nonlinear oscillator of van-der-Pol/FitzHugh-Nagumo type under quenched noise as a piecewise-deterministic Markov process. There are several interesting effects such as period shifts and new different trapped types of small-amplitude oscillations, which can be captured analytically. Furthermore, we numerically discover quenched resonance and show that it differs significantly from previous finite-noise optimality resonance effects. This demonstrates that quenched oscillators can be viewed as a new building block of nonlinear dynamics.*

Classical oscillators are of fundamental importance for many phenomena, either on an individual level [1, 2], or in a coupled-oscillator case for complex networked dynamics systems [3]. The most frequently encountered nonlinear oscillator are van der Pol [4] (or FitzHugh-Nagumo [5]) bistable systems, which have found applications in mechanical systems, neuroscience, lasers, electronics, chemistry, systems biology, geophysics, and many other areas, where multiscale hysteresis oscillation patterns are observed. Beyond classical hysteresis-type or relaxation oscillations [4], there are more complex oscillation patterns in forced oscillations such as mixed-mode oscillations (MMOs) [6] composed of small-amplitude oscillations (SAOs) and large-amplitude oscillations (LAOs). Furthermore, the influence of noise on oscillations has been a significant development, in-

cluding the description of effects such as stochastic resonance (SR) [7, 8], coherence resonance (CR) [9], self-induced stochastic resonance [10], steady-state stochastic resonance [11] and inverse stochastic resonance [12]; see [13] for a broad review of SR. The underlying, and unexpected, principle of these noise-induced resonances is that a *finite* noise strength optimizes the oscillation regularity. Yet, these effects have been developed and studied under the assumption of *annealed disorder*, leading to stochastic forces such as colored, white, or shot-noise [14]. There are also studies of annealed noise MMOs, e.g. [15, 16]. Here we consider the *quenched disorder* case for multiscale nonlinear oscillators. In fact, several stochastic effects are modelled by random parameters, which just change at certain time instances, rather than parameters fluctuating continuously. A simple example are mechanical systems involving random loading. A load usually does not change continuously but at certain time instances. Quenched disorder naturally leads to a piecewise-deterministic Markov process [17]. It also opens up new connections to uncertainty quantification [18] adding a fundamental nonlinear component for uncertainty propagation. We also remark that we study *quenched noise* in a single oscillator. Hence, this work is not directly connected to quenched *oscillation and amplitude death* [19], which are phenomena present already in (coupled) deterministic oscillator models; yet, it would be highly interesting if it is possible to establish potential connections in the future.

Our main results are three phenomena: period modulation for LAOs, two new types of SAOs, and the main novel effect of quenched resonance over a broad range of noises including start and termination effects. We provide analytical as well as numerical evidence for our results and show that the choice of quenched noise dis-

tribution can be very broad, illustrating the effects for the uniform, exponential and normal distributions; the results are easily adapted to far broader classes of distributions. In summary, this Letter demonstrates the broad potential for quenched oscillators as a new building block of nonlinear dynamics.

Setting: The prototypical example we are going to study is the quenched-random forced van der Pol oscillator

$$\frac{d^2x}{dt^2} + \mu(x^2 - 1)\frac{dx}{dt} + x = P(t, \omega), \quad (1)$$

where $x = x(t) \in \mathbb{R}$, $\mu > 0$ controls the (nonlinear) damping, we assume $\mu \gg 1$, and $P = P(t, \omega)$ is a quenched-random, time-dependent forcing, i.e., P is going to be fixed for time intervals $\mathcal{I}_j = [t_{j+1}, t_j) \subset [0, \infty)$ with $j \in \mathbb{N}$, and P switches randomly at the beginning of each time interval to a new value according to a given distribution. We set $(\Delta t)_j := t_{j+1} - t_j$ and assume true quenching, i.e., $t = \mathcal{O}(1)$, thereby avoiding any rapidly-switched forcing limits. The random forcing we consider can easily be implemented experimentally in mechanical systems. It also occurs naturally in neuroscience, where neuron model parameters are fixed for considerable time scales, yet may change due to internal or external events. The second-order equation (1) can be transformed via a standard Liénard ansatz

$$y := \frac{1}{\mu^2} \frac{dx}{dt} + \frac{1}{3}x^3 - x, \quad \varepsilon := 1/\mu^2, \quad s := t/\varepsilon,$$

into a fast-slow system ($0 < \varepsilon \ll 1$)

$$\begin{aligned} \varepsilon \frac{dx}{ds} &= \varepsilon \dot{x} = y - \frac{1}{3}x^3 + x =: f(x, y), \\ \frac{dy}{ds} &= \dot{y} = P - x =: g(x, y). \end{aligned} \quad (2)$$

Since $P = P(t, \omega) = P(\varepsilon s, \omega)$ and time intervals with $(\Delta t)_j = \mathcal{O}(1)$ yield $(\Delta s)_j = \mathcal{O}(1/\varepsilon)$, there are long epochs of order $\mathcal{O}(1/\varepsilon)$, where the system is completely deterministic on the slow time scale s . Of course, one may also re-write (2) on the fast time scale $t = s/\varepsilon$

$$\begin{aligned} \frac{dx}{dt} &= x' = y - \frac{1}{3}x^3 + x, \\ \frac{dy}{dt} &= y' = \varepsilon(P - x). \end{aligned} \quad (3)$$

We recall the fast-slow bifurcation analysis of the van der Pol oscillator to fix the notation [20]. The critical manifold is $\mathcal{C}_0 := \{(x, y) \in \mathbb{R}^2 : y = \frac{1}{3}x^3 - x =: h(x)\}$. It consists of steady states for the fast subsystem

$$\begin{aligned} x' &= y - \frac{1}{3}x^3 + x, \\ y' &= 0, \end{aligned} \quad (4)$$

obtained from (3) in the singular limit $\varepsilon \rightarrow 0$. \mathcal{C}_0 contains two fold points $p_{\pm} = (\pm 1, \mp 2/3)$, which separate the manifold into attracting parts $\mathcal{C}_0^{a-} = \mathcal{C}_0 \cap \{x < -1\}$, $\mathcal{C}_0^{a+} = \mathcal{C}_0 \cap \{x > 1\}$, and the repelling part $\mathcal{C}_0^r = \mathcal{C}_0 \cap \{-1 < x < 1\}$. The three parts are normally hyperbolic [21] and have the claimed stability properties for (4) since $\partial_x f(p) < 0$ for $p \in \mathcal{C}_0^{a\pm}$ and $\partial_x f(p) > 0$ for $p \in \mathcal{C}_0^r$. \mathcal{C}_0 can also be viewed as the phase space of the slow subsystem

$$\begin{aligned} 0 &= y - \frac{1}{3}x^3 + x, \\ \dot{y} &= P - x, \end{aligned} \quad (5)$$

which is a differential-algebraic equation (DAE) arising as the singular limit of (2). If $P \in \mathbb{R}$ is viewed as a *fixed deterministic parameter*, there are two fold bifurcations in the fast subsystem at $P = \pm 1$, which correspond to singular Hopf bifurcation points of the full system (2) [20]. In this context, the unique global steady state $(x^*, y^*) = (P, h(P))$ is globally stable for $|P| > 1$ and destabilizes at two singular Hopf bifurcations leading to large-amplitude relaxation oscillations via a canard explosion [22]. If $P(\cdot, \omega)$ is chosen randomly at multiple times t_j , then physical intuition and results from SR/CR suggest that oscillations can be *mixtures* of *near-stationary* and *oscillatory*. However, due to the quenching, the dynamical phase space geometry and statistical properties of these mixtures are very different from established phenomena. We are going to analyze quenched nonlinear oscillations in three steps: (I) random modulations of the period of relaxation oscillations (or pure LAOs), (II) generation of different types of SAOs, and (III) the analysis of resonance phenomena within MMOs.

(I) Quenched LAOs: We fix the duration between switches uniformly $(\Delta t)_j = (\Delta t)$ for all j ; other cases are possible but will not be discussed here. We assume P at t_j is sampled from a density $p = p(\omega)$, $\omega \in \mathbb{R}$. From standard fast-slow systems results [20], it follows that if the support of p is compact and properly contained in the interval $(-1, 1)$, then there exists $\varepsilon_0 > 0$ such that for all $\varepsilon \in (0, \varepsilon_0]$ we get standard relaxation oscillations; see also Figure 1(a). Yet, the *period* T will be a random variable $T = T(\omega)$ depending upon the chosen distribution $p = p(\omega)$. Since (2) remains invariant under the symmetry $x \mapsto -x$, $y \mapsto -y$, relaxation oscillations are symmetric so we assume for now $p(\omega) = p(-\omega)$. To leading-order $T = T_0 + \mathcal{O}(\varepsilon^{2/3})$ [23], where T_0 is approx-

imated by the slow drift on $\mathcal{C}_0^{\text{a}\pm}$ via the slow subsystem (5). Implicit time differentiation gives

$$\dot{y} = \dot{x}(x^2 - 1) \quad \Rightarrow \quad \dot{x} = \frac{P - x}{x^2 - 1}.$$

A Dorodnitsyn-type [23, 20] calculation yields

$$T = T_0 + \mathcal{O}(\varepsilon^{2/3}) \approx \int_2^1 \frac{x^2 - 1}{P - x} dx + \int_{-2}^{-1} \frac{x^2 - 1}{P - x} dx,$$

where we used a leading-order drop point approximation for the random starting point on $\mathcal{C}_0^{\text{a}\pm}$ by just setting $x_0(\omega) \approx \pm 2$ and dropped the perturbation term $\mathcal{O}(\varepsilon^{2/3})$. Working out the integral yields

$$T_0 = 2P^2 \coth^{-1}(2P + 3) + 2P^2 \coth^{-1}(3 - 2P) + \ln\left(\frac{P - 1}{P - 2}\right) - \ln\left(\frac{P + 2}{P + 1}\right) + 3 =: v(P).$$

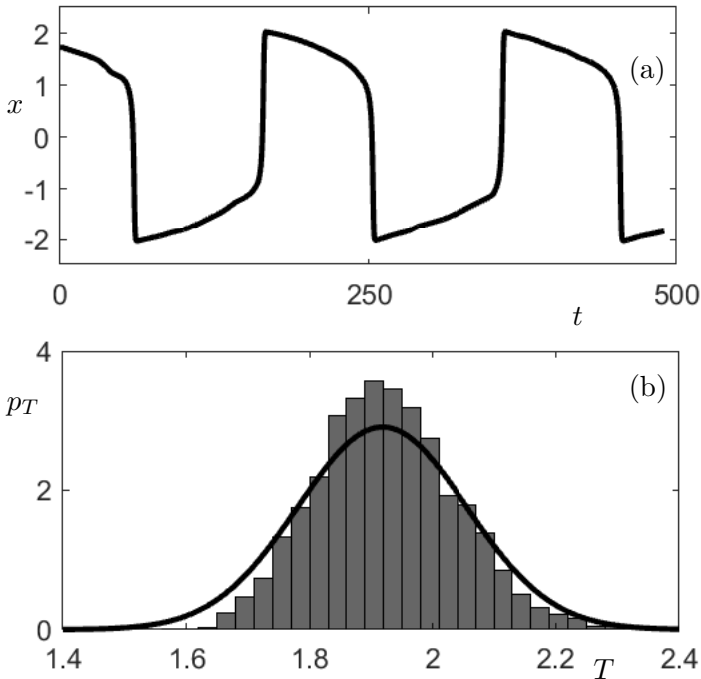


Figure 1: (a) x -time series of (2) drawn up to $T = 500$; full trajectory is of length $T = 5 \cdot 10^6$. Parameters are $\varepsilon = 0.01$, $l = 0.75$ and $(\Delta t) = 10$. (b) Modulated period histogram computed from the full trajectory shifted by $3.5 \cdot \varepsilon^{2/3}$; solid curve is a Gaussian density calculated from the analytical random Dorodnityn-type approximation.

Since $P \in (-1, 1)$ throughout this section, the function $v : (-1, 1) \rightarrow (v(-1), v(+1)) =: (q_-, q_+)$ is symmetric, i.e. $v(P) = v(-P)$. Furthermore, v is smooth and piecewise monotonic with $v' < 0$ for $P \in (-1, 0)$ and $v' > 0$ for $P \in (0, 1)$. So P having density p , gives that T has approximately density $q(y) = p(v^{-1}(y))(v^{-1})'(y)$, where the inverse is understood in a piecewise sense. Calculating v^{-1} explicitly is not possible, yet calculating centered moments is easy since

$$\begin{aligned} \langle (T - \mu)^k \rangle &= \int_{q_-}^{q_+} (y - \mu)^k p(v^{-1}(y)) v^{-1}'(y) dy \\ &= \int_{-1}^1 (v(\omega) - \mu)^k p(\omega) d\omega, \quad \mu := \langle T \rangle. \end{aligned}$$

Even for the basic distributions p , we get interesting results. Let $p_\delta(x) = \delta(x)$ be a point mass, let $p_{u,l}$ be a uniform distribution on $(-l, l)$ with $l \in (0, 1)$. Then $\mu_\delta = 3 - 2 \ln 2$ is the classical deterministic result. For the uniform case, the integrals can be evaluated explicitly, yet the formula is lengthy. The second-order Taylor polynomial near $l = 0$ of the explicit formula gives

$$p_{u,l} = (3 - 2 \ln(2)) + l^2 \left(\frac{\log(4)}{3} - \frac{1}{4} \right) + \mathcal{O}(l^4).$$

so the average period increases as the distribution broadens, which actually is an observation true irrespective of the Taylor approximation. One may easily evaluate the variance σ_u^2 , and higher-order moments, from the formulas above. For very long trajectories or relatively small (Δt) , we expect by Central Limit Theorem to obtain a normal distribution $T_0 \rightarrow \mathcal{N}(\mu_{u,l}, \sigma_{u,l})$; see Figure 1(b). We observe that the largest error in the calculation arises by neglecting the term $\mathcal{O}(\varepsilon^{2/3})$. Short/intermediate-term fluctuations are non-Gaussian for generic input distributions. In general, input noise in P gets *transformed* to noise in the period via a *nonlinear* mapping v .

(II) Quenched SAOs: Relaxation oscillations can also be completely blocked, despite quenched noise, in the case $P \in (-\infty, -1)$ or $P \in (1, \infty)$. We assume here $P \in (1, \infty)$, consider an initial condition on $\mathcal{C}_0^{\text{a}\pm}$ but $\varepsilon > 0$ and now take a shifted exponential density $p(\omega) = \frac{1}{\mu} e^{-(\omega-1)/\mu}$ for $\omega > 1$, and $p(\omega) = 0$ zero otherwise. A time series is shown in Figure 2.

We observe that there are *two* types of SAOs. On the one hand, we get small oscillations due to a stable spiral

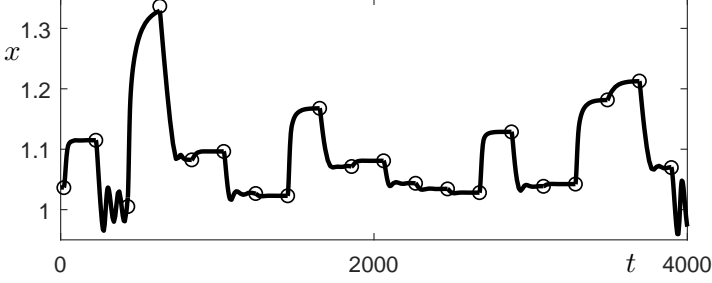


Figure 2: x -time series of (2) with $\varepsilon = 0.01$, and P drawn from the shifted exponential distribution with $\mu = 0.1$ and $(\Delta t) = 200$.

steady state for (2). The condition can be calculated by linearizing at $(x_*, y_*) = (P, h(P))$, considering the Jacobian J , and using the trace-determinant condition for complex eigenvalues

$$\text{trace}(J)^2 - 4 \det(J) < 0 \quad \Leftrightarrow \quad (1 - P^2)^2 < 4\varepsilon.$$

For our choice of exponential distribution, or similarly for other distributions, we now just have to calculate under the assumption that (Δt) is sufficiently large to track the equilibrium that

$$\begin{aligned} \mathbb{P}(\text{spiral SAO in } (t_j, t_{j+1})) &= \int_1^{\sqrt{1+\sqrt{4\varepsilon}}} \frac{1}{\mu} e^{-(\omega-1)/\mu} d\omega \\ &= 1 - e^{-\frac{1-\sqrt{2\sqrt{\varepsilon}+1}}{\mu}} = \frac{\sqrt{\varepsilon}}{\mu} + \frac{(-\mu-1)\varepsilon}{2\mu^2} + \mathcal{O}(\varepsilon^{3/2}). \end{aligned}$$

Therefore, there is a very fine balance between the time scale separation and the mean of the exponential distribution for small spiral SAOs.

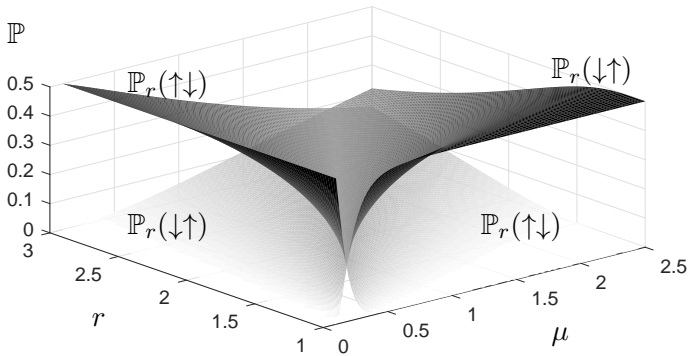


Figure 3: Probability of non-spiral half-rotation SAOs showing the two intersecting smooth surfaces $\mathbb{P}_r(\downarrow\uparrow)$ and $\mathbb{P}_r(\uparrow\downarrow)$.

If we just focus on SAOs without small spirals, then a good approximation is just to let $\varepsilon = 0$ and calculate

the shifting pattern of the random steady state $x_j^* = P(t_j, \omega) \in \mathcal{C}_0^{a+}$ for the slow subsystem (5). Let

$$\mathbb{P}_r(\downarrow\uparrow) := \mathbb{P}(x_{j+1}^* < x_j^*, x_{j+1}^* < x_{j+2}^* | x_j^* = r),$$

i.e., it is the probability that we start at level r , then move down slowly very close to the new steady state (assuming (Δt) is sufficiently large), and then moving up towards the next steady state. Hence, $\mathbb{P}_r(\downarrow\uparrow)$ is the probability to get a non-spiral half-oscillation SAO within $2(\Delta t)$. Similarly, we can define and interpret $\mathbb{P}_r(\uparrow\downarrow)$. We calculate for the exponential distribution case, setting $p_{1r} := \int_1^r p(\omega) d\omega$, that

$$\begin{aligned} \mathbb{P}_r(\downarrow\uparrow) &= \int_1^r p_{1r}(1 - p_{1s})p(s) ds \\ &= \frac{1}{2}e^{-\frac{3r}{\mu}} \left(e^{1/\mu} - e^{r/\mu} \right)^2 \left(e^{1/\mu} + e^{r/\mu} \right). \end{aligned}$$

Similarly, we calculate

$$\begin{aligned} \mathbb{P}_r(\uparrow\downarrow) &= \int_r^\infty (1 - p_{1r})p_{1s}p(s) ds \\ &= e^{-\frac{2-2r}{\mu}} - \frac{1}{2}e^{-\frac{3-3r}{\mu}}. \end{aligned}$$

Figure 3 shows the results as functions of r and μ . Similarly, one can also deal with more complex SAO sequences, and calculate the probabilities $\mathbb{P}_r(\uparrow\uparrow\downarrow)$, $\mathbb{P}_r(\downarrow\downarrow\uparrow)$, etc of patterns explicitly. If (Δt) is too small, we do not track the steady states and even more complex patterns arise, which are captured by the precise time evolution of the slow subsystem similar to situation for LAOs discussed above.

(III) Quenched Resonance: Instead of modulated relaxation oscillations, which can also be viewed as LAOs, and SAOs as discussed in the previous section, we can also expect *mixtures* of these under the influence of noise. In this section, we are sampling from a normal distribution $P \sim \mathcal{N}(\mu, \sigma^2)$.

Figure 4 shows examples of the possible dynamics. The mean steady state is located at $(x^*, y^*) = (\mu, h(\mu)) = (1.1, h(1.1))$ for our choice of parameters. Four different regimes can be observed upon increasing the noise level: (A) no LAOs/spikes but some SAOs as shown in Figure 4(a); (B) occasional LAOs interspersed with SAOs, i.e., MMOs occur as shown in Figure 4(b); (C) MMOs with more regular LAOs are displayed in Figure 4(c); (D) some large spikes but also long periods

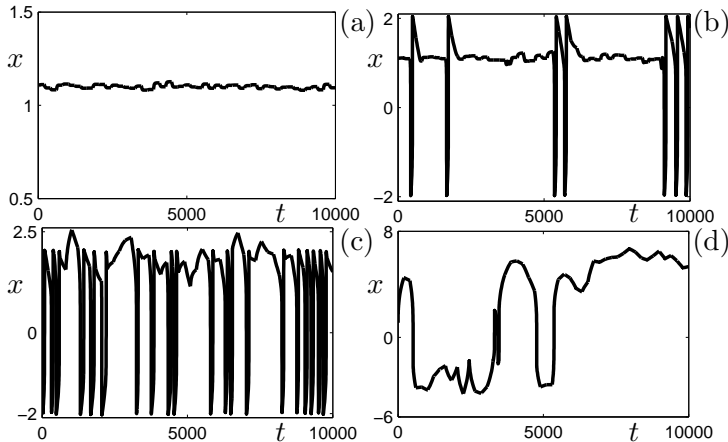


Figure 4: Time series with $\varepsilon = 0.01$, and P drawn from a Gaussian distribution with $\mu = 0.1$, and we fixed $(\Delta t) = 200$. (a) $\sigma = 0.01$. (b) $\sigma = 0.1$. (c) $\sigma = 1$. (d) $\sigma = 10$.

of random drift near the attracting branches \mathcal{C}_0^{\pm} are shown in Figure 4(d). To quantify the regularity of the oscillations, we use the noise-to-signal ratio known from SR/CR quantification [9, 24]

$$R = \frac{\sqrt{\langle \tau^2 \rangle - \langle \tau \rangle^2}}{\langle \tau \rangle},$$

where τ is the duration between two zero crossings of x with $x' > 0$ at the crossing.

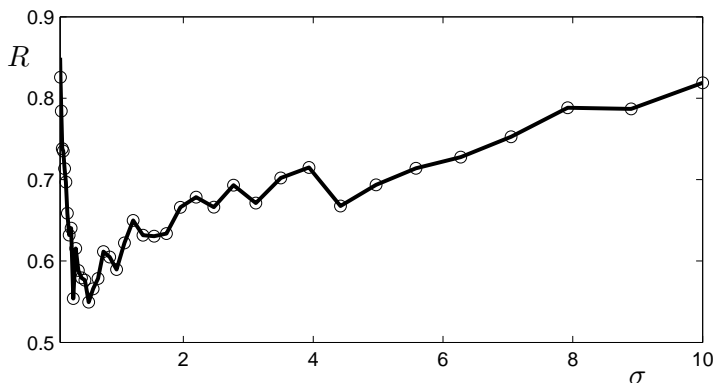


Figure 5: Standard deviation σ of the input forcing distribution versus noise-to-signal ratio. Parameters are $\varepsilon = 0.01$, $\mu = 0.1$, and $(\Delta t) = 200$. For the sampling we considered 20 sample paths of slow-time length $s = 1000$ on a logarithmically-spaced σ -space (indicated by circles), and interpolated the measurement points linearly.

Our intuition from Figure 4 is confirmed with detailed statistics of σ and R in Figure 5. For small noise level

σ , there are only rare excursions as the system mostly has a steady state on \mathcal{C}_0^+ . For a very broad range of intermediate noises, the behaviour improves as R decreases implying more regular LAOs, while for very large noise level, there is again a higher probability of getting trapped on either of the two branches \mathcal{C}_0^{\pm} for extended time periods. In particular, there is a finite *optimal noise level* for the input forcing, which we refer to as *quenched resonance*. There is some similarity to CR/SR/etc as one has to eliminate via noise a deterministically stable steady state. Yet there are substantial differences to CR/SR/etc. For low noise levels, there are *no* oscillations. Furthermore, there is a *much broader range of noises*, where an improved regular oscillation can be observed. Lastly, the termination mechanism does not lead to a purely noisy but to a two-stage *nearly trapped* piecewise-deterministic process.

Summary: We have shown that quenched disorder leads to new effects in the core class of multiscale nonlinear oscillators. This applies to slow scales for SAOs and to fast-slow scales for LAOs. We have proven that analytical calculations are possible and can be carried out for different random forcings. Furthermore, quenched resonance was discovered, which differs significantly from CR/SR. However, this Letter is clearly just a starting point for a far more general study of nonlinear multiscale dynamical systems under quenched disorder, on the individual as well as network level.

Acknowledgements: I would like to thank the VolkswagenStiftung for support via a Lichtenberg Professorship.

References

- [1] J. Guckenheimer and P. Holmes. *Nonlinear Oscillations, Dynamical Systems, and Bifurcations of Vector Fields*. Springer, New York, NY, 1983.
- [2] A.H. Nayfeh and D.T. Mook. *Nonlinear Oscillations*. Wiley, 1995.
- [3] S.H. Strogatz. Exploring complex networks. *Nature*, 410:268–276, 2001.
- [4] B. van der Pol. On relaxation oscillations. *Philosophical Magazine*, 7:978–992, 1926.

- [5] R. FitzHugh. Mathematical models of threshold phenomena in the nerve membrane. *Bull. Math. Biophysics*, 17:257–269, 1955.
- [6] M. Desroches, J. Guckenheimer, C. Kuehn, B. Krauskopf, H. Osinga, and M. Wechselberger. Mixed-mode oscillations with multiple time scales. *SIAM Rev.*, 54(2):211–288, 2012.
- [7] R. Benzi, A. Sutera, and A. Vulpiani. The mechanism of stochastic resonance. *J. Phys. A*, 14(11):453–457, 1981.
- [8] C. Nicolis and G. Nicolis. Stochastic aspects of climatic transitions—additive fluctuations. *Tellus*, 33(3):225–234, 1981.
- [9] A.S. Pikovsky and J. Kurths. Coherence resonance in a noise-driven excitable system. *Phys. Rev. Lett.*, 78:775–778, 1997.
- [10] C.B. Muratov, E. Vanden-Eijnden, and W. E. Self-induced stochastic resonance in excitable systems. *Physica D*, 210:227–240, 2005.
- [11] C. Kuehn. Time-scale and noise optimality in self-organized critical adaptive networks. *Phys. Rev. E*, 85(2):026103, 2012.
- [12] B.S. Gutkin, J. Jost, and H.C. Tuckwell. Inhibition of rhythmic neural spiking by noise: the occurrence of a minimum in activity with increasing noise. *Naturwissenschaften*, 96(6):1091–1097, 2009.
- [13] L. Gammaitoni, P. Hänggi, P. Jung, and F. Marchesoni. Stochastic resonance. *Rev. Mod. Phys.*, 70:223–287, 1998.
- [14] C. Gardiner. *Stochastic Methods*. Springer, Berlin Heidelberg, Germany, 4th edition, 2009.
- [15] N. Berglund and D. Landon. Mixed-mode oscillations and interspike interval statistics in the stochastic FitzHugh-Nagumo model. *Nonlinearity*, 25:2303–2335, 2012.
- [16] D.J.W. Simpson and R. Kuske. Mixed-mode oscillations in a stochastic, piecewise-linear system. *Physica D*, 240(14):1189–1198, 2011.
- [17] M.H. Davis. Piecewise-deterministic Markov processes: A general class of non-diffusion stochastic models. *J. R. Stat. Soc. B*, 46(3):353–388, 1984.
- [18] M. Grigoriu. *Stochastic Systems: Uncertainty Quantification and Propagation*. Springer, 2012.
- [19] A. Koseka, E. Volkov, and J. Kurths. Oscillation quenching mechanisms: Amplitude vs. oscillation death. *Phys. Rep.*, 531(4):173–199, 2013.
- [20] C. Kuehn. *Multiple Time Scale Dynamics*. Springer, 2015. 814 pp.
- [21] N. Fenichel. Geometric singular perturbation theory for ordinary differential equations. *J. Differential Equat.*, 31:53–98, 1979.
- [22] M. Diener. The canard unchained or how fast/slow dynamical systems bifurcate. *The Mathematical Intelligencer*, 6:38–48, 1984.
- [23] E.F. Mishchenko and N.Kh. Rozov. *Differential Equations with Small Parameters and Relaxation Oscillations (translated from Russian)*. Plenum Press, 1980.
- [24] B. Lindner and L. Schimansky-Geier. Analytical approach to the stochastic FitzHugh-Nagumo system and coherence resonance. *Phys. Rev. E*, 60(6):7270–7276, 1999.